Locally pH controlled and directed growth of supramolecular gel microshapes using electrocatalytic nanoparticles

Lakshminarayanan, Vasudevan; Poltorak, Lukasz; Bosma, Duco; Sudhölter, Ernst J.R.; Van Esch, Jan H.; Mendes, Eduardo

DOI
10.1039/c9cc04238e

Publication date
2019

Document Version
Accepted author manuscript

Published in
Chemical Communications

COMMUNICATION

Locally pH controlled and directed growth of supramolecular gel microshapes using electrocatalytic nanoparticles

Received 00th January 20xx,
Accepted 00th January 20xx

DOI: 10.1039/x0xx00000x

Vasudevan Lakshminarayanan,[a]‡ Lukasz Poltorak,*[a,b]‡ Duco Bosma,[a] Ernst J. R. Sudhölter,[a] Jan van Esch,[a] Eduardo Mendes**[a]

Controlled localization of platinum nanoparticles (Pt NPs) at the solid support assisted by the polarized liquid – liquid interface is reported. The electro-catalytic water oxidation resulted in the local pH modulation followed by directed self-assembly of Dibenzoyl-L-Cystine hydrogelator forming a structured hydrogel retaining the shape of Pt NPs deposit.

Supramolecular hydrogels have been reported to find applications in the fields of cell culturing,[1] drug delivery systems[2] among many others. The ability to exert spatial control over the formation of these materials is therefore of high value. Directed self-assembly of supramolecular hydrogelators composed of low molecular weight gelators has seen a rapid progress in recent years. With the ability to control supramolecular gel formation using pH or catalysts,[3,4] researchers have shown that spatial structuring at the microscale is possible by using light,[5] catalytic surfaces,[6] electrochemistry,[7,8] reaction-diffusion[9] and very recently, charged polymer brushes.[10] However, such approaches need the aid of masks to create patterns, secondary supporting networks to act as reservoirs for the gelator precursors or micro-contact printing to template micropatterns. Hence, new techniques allowing for localized control over hydrogel formation and structuring can pave the way for novel soft material fabrication and patterning. Electrochemical approaches for hydrogel study and formation established so far, although limited to only a few reports, have shown promise due to their ease of use, reversibility or multiplexing ability.[7,11,12] In this work, we take this approach to the next level by demonstrating localized control over hydrogel formation. This is achieved with the help of a polarized liquid-liquid interface to deposit Pt NPs on a conducting substrate of fluorine doped tin oxide (FTO) electrodes. The polarized liquid – liquid interface also known as the interface between two immiscible electrolyte solutions (ITIES) is soft, renewable, free from defects and allows the electrochemical study of interfacial ion or electron transfer processes. The liaison between ITIES and functional materials is a relatively new and unexplored topic.[13] The ion or electron transfer reactions or the self-assembly process can lead to interfacial region modification with a number of functional materials (*e.g.* molecular sieves, liquid mirrors, metal catalysts).[14–16] When the ITIES is contacted to conducting support the so-called three phase junction is formed. At the junction where the three phases meet, the interfacial ion transfer coupled to a redox reaction can result in very precise electrochemical deposition (*e.g.* the formation of Au NPs or silica).[17–19] In this work, we have employed this property to make patterned (rings, stripes and spots) hydrogels by controlled formation of Pt NPs that will act as catalyst for the electrochemical splitting of water to produce a proton gradient. Controlled and localized Pt NPs deposition at the micro-meter scale is facilitated by the ITIES (micro-capillary supported liquid – liquid interface or by a three phase junction system). The proton gradient thus produced causes the self-assembly of the hydrogelator Dibenzoyl-L-Cystine (DBC). For simplicity, we have chosen an off-the shelf gelator as a model molecule. We believe that this technology platform gives solid foundation for future electrochemically assisted deposition and writing of supramolecular hydrogels.

First, we focus on the demonstrations that an electro-catalytic effect of Pt NPs on hydrogel formation occurs. The FTO electrode placed in an electrochemical cell (experimental details are available in section 2.1 of the SI) was contacted via a circular opening to a 1 mM aqueous solution of K_2PtCl_6 and the Pt NPs were deposited via chronoamperometry for a period of 10 min. The potential applied (E = – 1.5 V *vs* Ag/AgCl) was sufficient to reduce $PtCl_6^{2-}$ to metallic Pt according to reaction 1 and 2:

$$Pt^{IV}Cl_6^{2-} + 2e^- \rightarrow Pt^{II}Cl_4^{2-} + 2Cl^- \quad (1)$$

$$Pt^{II}Cl_4^{2-} + 2e^- \rightarrow Pt^0 + 4Cl^- \quad (2)$$

Fig. 1B shows the FTO electrode decorated with a dark circle containing Pt NPs. Investigation by scanning electron microscopy (SEM) revealed that the deposited Pt NPs are well dispersed over the support and that their size range from 100 to 200 nm (see Fig. 1C and ESI 5B). Additional characterization by X-ray photoelectron

[a] *Delft University of Technology, Department of Chemical Engineering, Van der Maasweg 9, 2629 HZ Delft, The Netherlands*
[b] *University of Lodz, Faculty of Chemistry, Department of Inorganic and Analytical Chemistry, Electroanalysis and Electrochemistry Group, Tamka 12, 91-403 Lodz, Poland*

† These authors contributed equally
* Lukasz.poltorak@chemia.uni.lodz.pl; l.poltorak@tudelft.nl
** e.mendes@tudelft.nl

Electronic Supplementary Information (ESI) available: [methods and materials, protocols of organic salts preparation, details pertaining to electrochemical set-ups, water – 1.2-dichloroethane partition coefficient calculations, additional XPS, SEM and TEM results]. See DOI: 10.1039/x0xx00000x

spectroscopy (XPS) (see Fig. ESI 4) confirmed the presence of metallic Pt. The cyclic voltammograms recorded in aqueous 250 mM $NaNO_3$ before (red line in Fig. 1A) and after deposition of Pt NPs (black line in Fig. 1A) show a clear electro-catalytic effect towards water oxidation. For the latter, the anodic current recorded at 1.5 V was 115 times higher as compared to a non-modified FTO electrode having the same planar surface area. Two additional cathodic peaks recorded around 0.32 V and – 0.26 V are typical fingerprints of oxygen reduction and H^+ adsorption to the Pt electrodes, respectively.[20] The Pt NPs deposited on the FTO substrate were then used for the electrochemically assisted hydrogel deposition experiments. An aqueous 40 mM solution of the sodium salt of the DBC gelator with additionally 250 mM $NaNO_3$ as supporting electrolyte was used. Linear sweep voltammetry was carried out at a scan rate of 10 mV·s^{-1} with the forward polarization towards more anodic potential (typically the experiment was stopped between 2.5 – 3.0 V) and the polarized optical microscopy (POM) was used *in situ* to follow the changes at the surface of the FTO electrode. It is known that DBC gel fibers orient themselves along the diffusion gradient of the protons,[21] and hence, their presence can be followed and confirmed using POM. In Fig. 1D is shown the POM image of the FTO electrode modified with Pt NPs. The boundary between the Pt NPs modified and non-modified region is observed by microscopy as is indicated by the red line (inset in Fig. 1D). The application of a linear increasing anodic potential triggers the water oxidation reaction:

$$2H_2O - 4e^- \rightarrow 4H^+ + O_2 \quad (3)$$

As the local concentration of H^+ increases, we can observe the emergence of the DBC hydrogel (see Fig. 1E together with inset). From the image recorded we conclude that: (i) the hydrogel is built from DBC fibres and structured by the linear diffusion of protons from the support; (ii) in some of the regions of the support the emergence of so-called Maltese cross patterns indicate the radial orientation of the fibres, which in turn may suggest the presence of the isolated Pt NPs clusters or preferential electro-catalytic sites (behaving as the individual nano-electrodes).[22] The presence of DBC fibres was further confirmed by using Cryo-transmission electron microscopy investigations on electrochemically modified copper grids (see Fig. ESI 9 with the corresponding description) decorated with Pt NPs and clearly showed the formation of fibers growing from the Pt NPs surface. In order to control the local deposition of Pt NPs we combined the $PtCl_6^{2-}$ (initially present in the organic phase) transfer reactions across the electrified liquid – liquid interface with its reduction occurring at the FTO. First, we synthesized the organic phase soluble salt – $PtCl_6(BTPPA)_2$ *via* a simple metathesis reaction (see section 1.3 in ESI for details). We then studied its electrochemical behaviour at the ITIES in a typical four electrode configuration as described in section 2.2 of the ESI. We expected to find proof of principle that there is a transfer of $PtCl_6^{2-}$. In Fig. 2A shows the ion transfer voltammogram recorded at the interface between the aqueous 10 mM NaCl and 10 mM BTPPATPBCl (hydrophobic salt) dissolved in the 1,2-dichloroethane (the organic phase). The observed potential window is limited by $Na^+_{aq\leftrightarrow org}$ and $Cl^-_{aq\leftrightarrow org}$ transfer on the more and less positive potential sites, respectively. Addition of $PtCl_6(BTPPA)_2$ at µM concentration to the organic phase results in the emergence of two peaks with $E_{1/2}$ = 0.25 V within the available potential window (Fig. 2B). The positive peak is attributed to the $PtCl^{2-}_{6,org\rightarrow aq}$. The ratio of the integrated positive and negative signals approaching unity indicate the reversibility of the process.

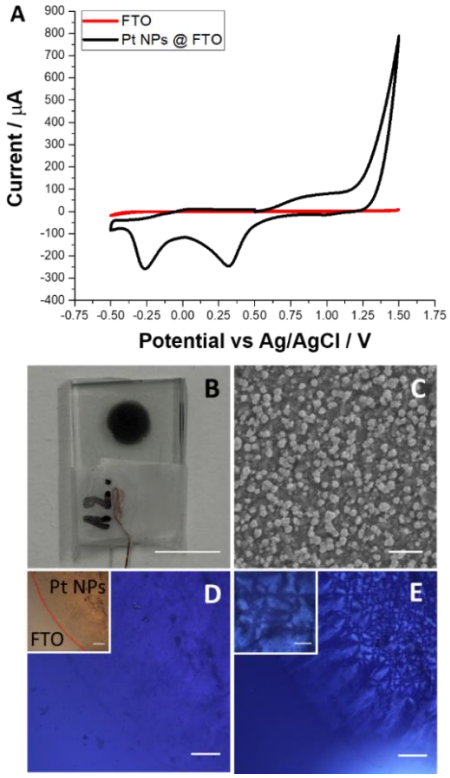

Figure 1. A – Cyclic voltammograms recorded in an aqueous solution of 250 mM $NaNO_3$ before (red) and after (black) Pt NPs deposition at -1.5V via a single step chronoamperometry for 10 min. **B** – is the photo of the corresponding, modified electrode. **C** – shows a SEM image of the area containing Pt NPs. **D** – is the optical microscopy image of the Pt NPs deposited (before hydrogel formation) on FTO under cross-polarized condition (inset shows image under normal light conditions with the boundary of Pt NPs indicated). **E –** is the optical microscopy image recorded under cross-polarization, after hydrogel formation the same FTO surface section is shown in D and E). The inset shows the Maltese cross-hair pattern zoomed in further. Scale bars are: B – 5 mm; C – 1 µm; D, D inset and E – 200 µm; E inset – 100 µm.

In Fig. 2C shows the recordings when the organic phase contained only 5 mM $PtCl_6(BTPPA)_2$ (the concentration used in further experiments) and shows the potential window, which is now limited on the negative potential side by the $PtCl^{2-}_{6,aq\leftrightarrow org}$. The concept of a three phase junction modification was mainly studied in the group of Opallo, where Au NPs or silica material were electrochemically generated in a defined locus.[17–19] To the best of our knowledge, this is the first time that the three phase junction is decorated with Pt NPs. The modification follows a few mutually related ion and electron transfer reactions that are depicted together with the electrical scheme in Fig. 3. First the reductive potential is applied to the FTO electrode and the $PtCl_6^{2-}$ present in the organic phase undergoes a reduction to metallic Pt (according to reaction 1 and 2) at the three phase junction. For an applied potential (*E* = – 1.5V) its reduction in the organic phase is unlikely due to very high resistance of the circuit (high resistivity of the organic phase and the position of the reference electrode), and is therefore excluded. The Cl^- formed within the junction or on the organic side of the ITIES will partition to the aqueous phase due to its high intrinsic hydrophilicity:

$$Cl^-_{\text{ITIES or org}} \rightarrow Cl^-_{aq} \quad (4)$$

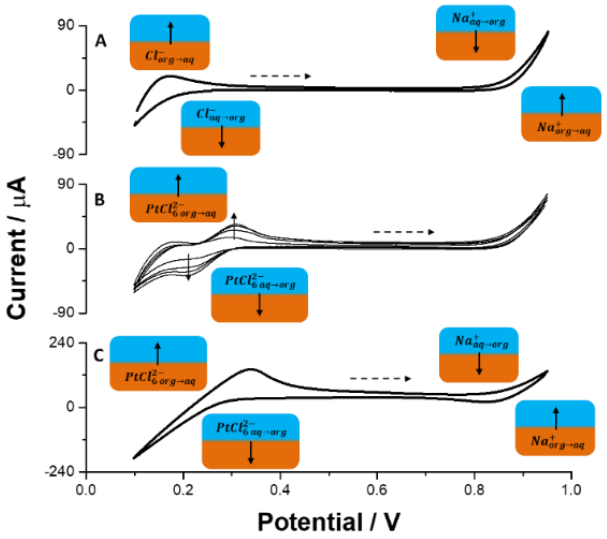

Figure 2. Ion transfer voltammograms recorded at the Liquid-liquid Interface formed between **A** – 10 mM NaCl (aq) // 10 mM BTPPATPBCl (org); **B** – 10 mM NaCl (aq) // x µM (x = 58; 116; 174 and 232 µM) $BTPPA_2PtCl_6$ in 10 mM BTPPATPBCl (org) and **C** – 10 mM NaCl (aq) // 5 mM $BTPPA_2PtCl_6$ (org). Scan rate was 10 mVs^{-1}; dashed arrow indicate the direction of the forward scan.

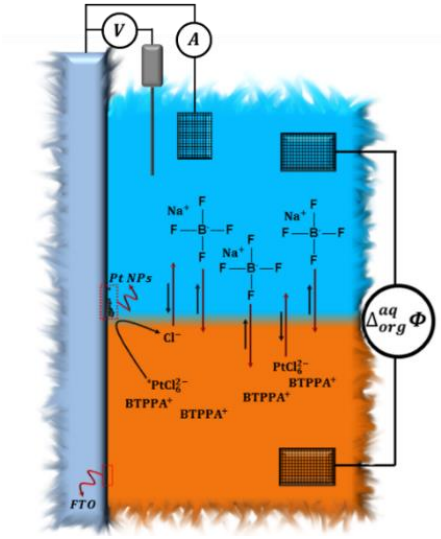

Figure 3. Schematic representation of the three phase junction system. Organic phase is 1.2-dichloroethane. For details refer to text.

In order to maintain the charge balance the anion (still soluble in the aqueous phase and significantly less hydrophilic than Cl^-) from the aqueous phase should transfer to the organic phase. This was provided with unidirectional BF_4^- transfer:

$$\mathrm{BF}_{4,\mathrm{aq}}^- \rightarrow \mathrm{BF}_{4,\mathrm{org}}^- \qquad (5)$$

As confirmed with the control experiment, in the absence of a charge balancing ion, the reaction 1, 2 and 4 will not occur and no deposit will be found (data not shown). Although $PtCl_6^{2-}$ is more hydrophobic than BF_4^- ($logP^0_{DCE,BF_4^-}$ = 3.4[23] < $logP^0_{DCE,PtCl_6^{2-}}$ = 5.1 – as calculated in section 3 of the ESI) we found that for experimental concentrations of $[BF^-_{4,aq}]$ = 100 mM and $[PtCl_6^{2-}]$ = 5 mM the latter was partitioning from the organic to the aqueous phase (clear colour change of the aqueous phase was observed over time):

$$\mathrm{PtCl}_{6,\mathrm{org}}^{2-} \rightarrow \mathrm{PtCl}_{6,\mathrm{aq}}^{2-} \qquad (6)$$

Whenever the $PtCl_6^{2-}$ will diffuse towards the cathodically polarized FTO electrode the reaction 1 and 2 will occur. To demonstrate the control over directed self-assembly of hydrogelators, different configurations of FTO substrate and liquid-liquid interface were made (see Fig. 4, row A). The detailed experimental information can be found in sections 2.2 – 2.5 of the ESI. Three designs were implemented to control the localization of Pt NPs: i) design where the conductive substrate was dipped into the organic phase (solution of 5 mM $BTPPA_2PtCl_6$ in 1,2-DCE) and contacted with the aqueous phase on top (Fig. 4 – A1) ; ii) design where a micro-droplet of the organic phase containing 5 mM $BTPPA_2PtCl_6$ is casted on top of the FTO substrate (Fig. 4 – A2); iii) design where a micro-capillary filled with the organic phase is positioned close to the FTO substrate (Fig. 4 – A3).

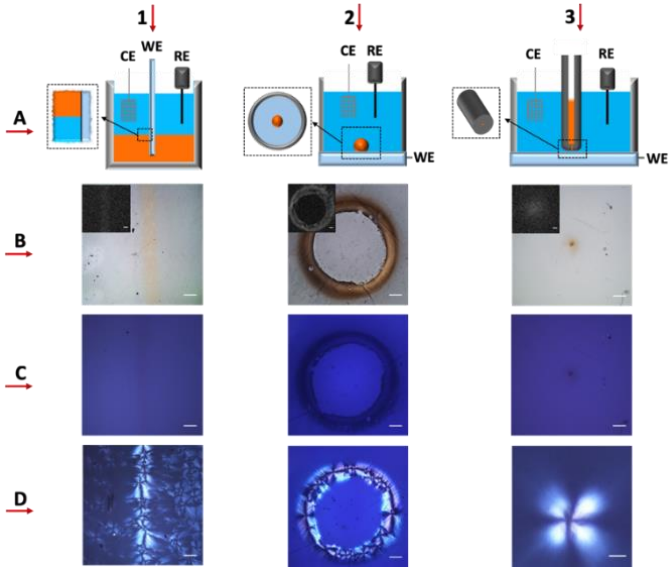

Figure 4. Three configurations used for localized Pt NPs deposition **1A** – scheme of a three phase junction for stripe deposition; **1B** – scheme of a three phase junction for ring deposition and **1C** – scheme of a micro-capillary supporting ITIES for micro-spot deposition. **Panel B** correspond to optical microscopy images (insets show the Energy Dispersive X-ray Spectrocopy mapping of Pt). **Panels C and D** represent polarization microscopy images before and after hydrogel deposition, respectively. The columns 1, 2 and 3 shows the results for stripe, ring and micro-spot respectively. Scale Bars are: 100 µm (left to right, B1 - B3, C1 - C3, D1 - D2) and 50 µm (D3) respectively.

In the first two designs, the formation of Pt NPs occurs at the three-phase junction while in the third design, this junction is absent and the Pt NPs are produced by transfer of $PtCl_6^{2-}$ from the organic to aqueous phase followed by its reduction at the FTO substrate. The Pt NPs reach micro-patterns that result from the designs are in the form of a stripe (*ca* 175 µm) , ring (*ca* 1.5mm diameter, 225 µm thick rim) and a spot (*ca* 60 µm diameter) respectively (Fig. 4 panel B). It was also observed that the width of the pattern was dependent on the deposition time (data not shown). The presence of the Pt NPs

was confirmed in all three cases via SEM (ESI Fig. 8) in combination with EDS elemental mapping (inset Fig. 4 row B).

The formation of hydrogels from these patterns was carried out using linear sweep voltammetry (see section 2.6 of ESI). It can be seen (Fig. 4 image 1D, 2D and 3D) that there is birefringence under cross-polarization indicating formation of oriented fibres. The time evolution of the hydrogel pattern together with a linear sweep voltammogram is shown in ESI Fig. 10. From the nature of the polarization pattern, it can be concluded that the DBC fibres are oriented radially outward based on the diffusion of the protons (towards a bulk phase) produced at the interface of Pt NP catalyst and the aqueous gelator environment. The produced hydrogels retain their shape of the base micro-pattern while being broader. Especially interesting is the hydrogel deposition obtained over a micro-spot as shown in Fig. 4 panel 3. As the region filled with Pt NPs has micrometre size, it resembles a single microdisc electrode, at which the mass transport (to and from the electrode) will be governed by a hemispherical diffusion. Very prominent and clear Maltese cross patterns indicate that the formed hydrogel has radial orientation and probably dome-like shape. This observation is in line with similar hemispherical shapes of silica,[24–26] metallic[27] or polymeric[28] deposits obtained over an array of nano- and micro-electrodes.

Electrochemically controlled Pt NPs deposition proposed in this work was used to produce sophisticated hydrogel patterns by combining them with supramolecular hydrogelators. Polarized liquid – liquid interface was used to control localization of Pt NPs, thereby creating new opportunities to design complicated and unusual gel patterns in a very straightforward manner. The electro-catalytic effect of Pt NPs towards water oxidation allowed the local pH change that triggered the growth of structured hydrogel directly from the support. Electrochemical patterning of hydrogels using the technique developed in this work can be used as a platform to create functional soft matter down to micro- or nano-metre scale. As such, it opens new gel processing directions with potential applications in cell culturing, drug delivery, tissue engineering, sensing, diagnostics *etc.* Such an approach may be used to produce nano-patterned electro responsive surfaces capable of templating hydrogels and other functional soft materials.

Conflicts of interest

There are no conflicts to declare.

Acknowledgements

The authors thank NanoNextNL (a Dutch consortium of 130 companies, universities, knowledge institutes and university medical centres) Program 7A for funding. The authors thank Bart Boshuizen for his help with XPS characterization.

Notes and references

1 V. Jayawarna, M. Ali, T. A. Jowitt, A. F. Miller, A. Saiani, J. E. Gough and R. V. Ulijn, *Adv. Mater.*, 2006, **18**, 611–614.
2 A. Friggeri, B. L. Feringa and J. van Esch, *J. Control. Release*, 2004, **97**, 241–8.
3 J. Boekhoven, J. M. Poolman, C. Maity, F. Li, L. van der Mee, C. B. Minkenberg, E. Mendes, J. H. van Esch and R. Eelkema, *Nat. Chem.*, 2013, **5**, 433–7.
4 F. Trausel, F. Versluis, C. Maity, J. M. Poolman, M. Lovrak, J. H. Van Esch and R. Eelkema, , DOI:10.1021/acs.accounts.6b00137.
5 C. Maity, W. E. Hendriksen, J. H. van Esch and R. Eelkema, *Angew. Chemie*, 2015, **127**, 1012–1015.
6 A. G. L. Olive, N. H. Abdullah, I. Ziemecka, E. Mendes, R. Eelkema and J. H. van Esch, *Angew. Chemie Int. Ed.*, 2014, **53**, 4132–4136.
7 Y. Liu, E. Kim, R. V. Ulijn, W. E. Bentley and G. F. Payne, *Adv. Funct. Mater.*, 2011, **21**, 1575–1580.
8 J. Raeburn, B. Alston, J. Kroeger, T. O. McDonald, J. R. Howse, P. J. Cameron and D. J. Adams, *Mater. Horiz.*, 2014, **1**, 241–246.
9 M. Lovrak, W. E. J. Hendriksen, C. Maity, S. Mytnyk, V. van Steijn, R. Eelkema and J. H. van Esch, *Nat. Commun.*, 2017, **8**, 15317.
10 Y. Wang, S. Oldenhof, F. Versluis, M. Shah, K. Zhang, V. van Steijn, X. Guo, R. Eelkema and J. H. van Esch, *Small*, 2019, 1804154.
11 E. R. Cross and D. J. Adams, *Soft Matter*, 2019, **15**, 1522–1528.
12 M. Zelzer and R. V Ulijn, *Chem. Soc. Rev.*, 2010, **39**, 3351–7.
13 L. Poltorak, A. Gamero-Quijano, G. Herzog and A. Walcarius, *Appl. Mater. Today*, 2017, **9**, 533–550.
14 L. Poltorak, K. Morakchi, G. Herzog and A. Walcarius, *Electrochim. Acta*, 2015, **179**, 9–15.
15 E. Smirnov, P. Peljo, M. D. Scanlon, F. Gumy and H. H. Girault, *Nanoscale*, 2016, **8**, 7723–7737.
16 T. J. Stockmann, L. Angel, V. Brasiliense, C. Combellas and F. Kanoufi, *Angew. Chemie Int. Ed.*, 2017, **56**, 13493–13497.
17 J. Niedziolka and M. Opallo, *Electrochem. Commun.*, 2008, **10**, 1445–1447.
18 I. Kaminska, M. Jonsson-niedziolka, A. Kaminska, M. Pisarek, R. Ho, M. Opallo and J. Niedziolka-jonsson, *J. Phys. Chem. C*, 2012, **116**, 22476–22485.
19 I. Kaminska, J. Niedziolka-jonsson, A. Roguska and M. Opallo, *Electrochem. commun.*, 2010, **12**, 1742–1745.
20 D. Huang, B. Zhang, J. Bai, Y. Zhang, G. Wittstock, M. Wang and Y. Shen, *Electrochim. Acta*, 2014, **130**, 97–103.
21 I. Ziemecka, G. J. M. Koper, A. G. L. Olive and J. H. van Esch, *Soft Matter*, 2013, **9**, 1556.
22 D. W. M. Arrigan, *Analyst*, 2004, **129**, 1157–1165.
23 M. Suzuki, S. Kihara, K. Maeda, K. Ogura and M. Matsui, *J. Electroanal. Chem.*, 1990, **292**, 231–244.
24 Y. Liu, A. Holzinger, P. Knittel, L. Poltorak, A. Gamero-Quijano, W. D. a. W. D. A. W. D. a Rickard, A. Walcarius, G. G. Herzog, C. Kranz and D. W. M. M. D. W. M. Arrigan, *Anal. Chem.*, 2016, **88**, 6689–6695.
25 L. Poltorak, G. Herzog and A. Walcarius, *Langmuir*, , DOI:10.1021/la501938g.
26 A. Holzinger, G. Neusser, B. J. J. Austen, A. Gamero-Quijano, G. Herzog, D. W. M. Arrigan, A. Ziegler, P. Walther and C. Kranz, *Faraday Discuss.*, 2018, **210**, 113–130.
27 C. Zhu, G. Meng, Q. Huang, Z. Li, Z. Huang, M. Wang and J. Yuan, *J. Mater. Chem.*, 2012, **22**, 2271–2278.
28 Y. Sakurai, S. Okuda, H. Nishiguchi, N. Nagayama and M. Yokoyama, *J. Mater. Chem.*, 2003, **13**, 1862–1864.

